

Theory of the Hall Coefficient and the Resistivity on the Layered Organic Superconductors κ -(BEDT-TTF)₂X

Hiroshi KONTANI^{1,2} * and Hiori KINO²

¹ Theoretische Physik III, Universitaet Augsburg D-86135 Augsburg, Germany.

² Institute for Solid State Physics, University of Tokyo, Kashiwanoha, Kashiwa-shi, 277-8581, Japan.

(May 20, 2019)

In the organic superconducting κ -(BEDT-TTF)₂X compounds, various transport phenomena exhibit striking non-Fermi liquid behaviors, which should be the important clues to understanding the electronic state of this system. Especially, the Hall coefficient (R_H) shows Curie-Weiss type temperature dependence, which is similar to that of high- T_c cuprates. In this paper, we study a Hubbard model on an anisotropic triangular lattice at half filling, which is an effective model of κ -(BEDT-TTF)₂X compounds. Based on the fluctuation-exchange (FLEX) approximation, we calculate the resistivity (ρ) and R_H by taking account of the vertex corrections for the current, which is necessary for satisfying the conservation laws. Our theoretical results $R_H \propto T^{-1}$ and $\cot\theta_H \propto T^2$ explain the experimental behaviors well, which are unable to be reproduced by the conventional Boltzmann transport approximation. Moreover, we extend the standard Eliashberg's transport theory and derive the more precise formula for the conductivity, which becomes important at higher temperatures.

PACS numbers: 74.70.Kn, 72.10.-d, 74.20.-z, 75.50.Ee

I. INTRODUCTION

It is well-known that the superconducting organic compound κ -(BEDT-TTF)₂X systems exhibit rich variety of ground states, through the strong correlation effects between electrons¹. For example, X=Cu[N(CN)₂]Cl salt is in the antiferromagnetic (AF) insulating phase in a low pressure region, $P < 200$ bar. With increasing the pressure, it changes to the superconducting (SC) phase at the transition temperature $T_c = 13$ K through the weak first-order transition, and the SC phase disappears under $P \gtrsim 10$ kbar. Above T_c , $1/T_1 T \propto T^{-1}$ is observed for a wider range of temperatures, which reflects the growth of the AF fluctuations as the temperature decreases². Thus, it is natural to consider that the AF fluctuation is the origin of superconductivity.

Recently, several theoretical works on κ -(BEDT-TTF)₂X system were done by using the fluctuation-exchange (FLEX) approximation, which is a kind of self-consistent spin-fluctuation theory. They showed that the *d*-wave like superconductivity is induced by the strong AF fluctuations³⁻⁶. Moreover, characteristic features of the experimental pressure-temperature phase diagram were reproduced well^{3,6}.

In this system, various transport phenomena above T_c also show interesting non-Fermi liquid behaviors. Recently, the temperature dependence of the resistivity (ρ) and the Hall coefficient (R_H) for X=Cu[N(CN)₂]Cl were measured precisely above T_c under $P = 4.5 \sim 10$ kbar in Ref.⁷. According to the measurement, the approxi-

mate relations $\rho \propto T$ and $R_H \propto T^{-1}$ are observed for $T = 30 \sim 100$ K, and the Hall angle $\cot\theta_H \equiv (\sigma_{xx}/\Delta\sigma_{xy})$ is proportional to T^2 well. In other measurement on X=Cu[NCS]₂, R_H increases by a factor of three on cooling below 60K at ambient pressure ($T_c = 10$ K)⁸. The mechanism of these interesting non-Fermi liquid behaviors, which are also observed in high- T_c cuprates, should be understood consistently.

In this paper, we present the theoretical study on both ρ and R_H for κ -(BEDT-TTF)₂X by using the FLEX approximation. Based on the conserving approximation, all the vertex corrections (VC's) for the current which is necessary to satisfy conserving laws are taken into account. We find that the Curie-Weiss like behavior of R_H is naturally reproduced by the VC's when the AF fluctuations are dominant. On the other hand, the conventional Boltzmann approximation, which does not include any VC's, fails to reproduce the temperature dependence of R_H . Experimentally, an intimate relation between the AF fluctuations and the transport phenomena is recognized⁷.

Note that the effect of VC's in nearly AF Fermi liquid was first studied in high- T_c cuprates by refs.⁹ and¹⁰, and the overall behavior of R_H are naturally reproduced both for hole-doped compounds and for electron-doped compounds. The present study is based on them basically.

*present address: Department of Physics, Saitama University, 255 Shimo-Okubo, Urawa-city, 338-8570, Japan.

II. ELECTRONIC STATES GIVEN BY THE FLEX APPROXIMATION

We study the triangular lattice Hubbard model with anisotropic hopping parameters (t, t') as shown in the inset of Fig. 1, which is a simple effective model for κ -(BEDT-TTF)₂X system¹¹. The dispersion is given by

$$\epsilon_{\mathbf{k}}^0 = 2t(\cos(k_x) + \cos(k_y)) + 2t' \cos(k_x + k_y), \quad (1)$$

where we put the lattice spacing 1. We analyze this model by using the FLEX method, which is a kind of self-consistent perturbation theory. This method had been applied to the study of high- T_c cuprates, and various non-Fermi liquid behaviors were reproduced well^{12–14}. It has also been applied to the superconducting ladder compound, $\text{Sr}_{14-x}\text{Ca}_x\text{Cu}_{24}\text{O}_{41}$ ¹⁵.

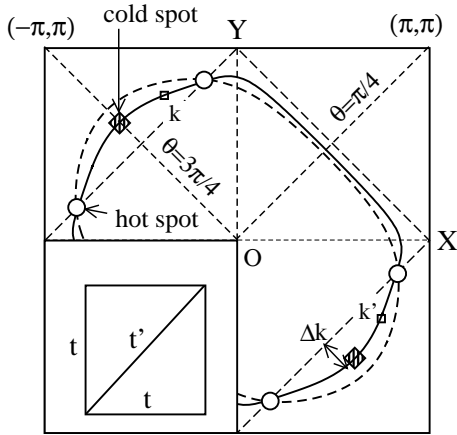


FIG. 1. The Fermi surface of the present model ($t'/t = 0.7$) for $U = 9$ (full line) and $U = 0$ (broken line) determined by $\text{Re}\{G_{\mathbf{k}}^{-1}(0)\} = 0$. The long-dashed lines, connecting between X and Y for example, represent the AF-zone boundary. The hot spots locate on the AF-zone boundary. Inset: the lattice structure.

In the present study we put $t = 1$ and $t' = 0.7$, where a d -wave like superconductivity is realized at $T_c > 0.02$ for $U \geq 7$, and it is replaced by the AF phase for $U \geq 10^3$. Figure 1 shows the Fermi surfaces at half-filling for $U = 0$ and $U = 9.0$ at $T = 0.02$. The Fermi surface is hole-like because $t, t' > 0$. There are two reflection symmetries with respect to the $(\theta = \pi/4)$ -axis and the $(\theta = 3\pi/4)$ -axis in Fig. 1. We see that the nesting of the Fermi surface is strengthened by the deformation of the Fermi surface in the case of finite U , which is caused by the real part of the self-energy.

The self-energy in the FLEX approximation is given by

$$\Sigma_{\mathbf{k}}(\epsilon_n) = T \sum_{\mathbf{q}, l} G_{\mathbf{k}-\mathbf{q}}(\epsilon_n - \omega_l) \cdot V_{\mathbf{q}}(\omega_l), \quad (2)$$

$$V_{\mathbf{q}}(\omega_l) = U^2 \left(\frac{3}{2} \chi_{\mathbf{q}}^s(\omega_l) + \frac{1}{2} \chi_{\mathbf{q}}^c(\omega_l) - \chi_{\mathbf{q}}^0(\omega_l) \right), \quad (3)$$

$$\chi_{\mathbf{q}}^{s(c)}(\omega_l) = \chi_{\mathbf{q}}^0(\omega_l) \cdot \{1 - (+)U\chi_{\mathbf{q}}^0(\omega_l)\}^{-1}, \quad (4)$$

$$\chi_{\mathbf{q}}^0(\omega_l) = -T \sum_{\mathbf{k}, n} G_{\mathbf{q}+\mathbf{k}}(\omega_l + \epsilon_n) G_{\mathbf{k}}(\epsilon_n), \quad (5)$$

where $\epsilon_n = (2n + 1)i\pi T$ and $\omega_l = 2l \cdot i\pi T$, respectively. By noticing the Dyson equation $\{G_{\mathbf{k}}(\epsilon_n)\}^{-1} = \epsilon_n + \mu - \epsilon_{\mathbf{k}}^0 - \Sigma_{\mathbf{k}}(\epsilon_n)$, we solve the eqs. (2)-(5) self-consistently, choosing the chemical potential μ so as to keep the system at half-filling. Here we use 4096 k -meshes and 256-Matsubara frequencies, respectively.

Here, $\chi_{\mathbf{q}}^s(0)$ gives the static spin susceptibility. Figure 2 shows the Curie-Weiss behavior of the maximum value of $\chi_{\mathbf{q}}^s(0)$, which is proportional to the square of the AF-correlation length ξ_{AF} . The obtained relation $\xi_{\text{AF}}^2 \propto T^{-1}$ is known to be caused by the renormalization of the self-energy. The FLEX approximation also gives the relation $(T_1 T)^{-1} = \sum_{\mathbf{k}} \text{Im}\chi_{\mathbf{k}}^s(\omega)/\omega \propto T^{-1}$.

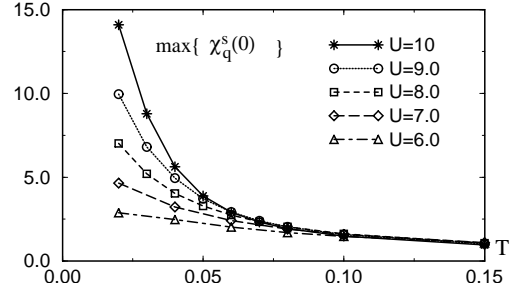


FIG. 2. The maximum value of $\chi_{\mathbf{q}}^s(0)$ ($\propto \xi_{\text{AF}}^2$) for $U = 6 \sim 10$.

Nonetheless $\chi_{\mathbf{q}}^s(0)$ for $U = 0$ is incommensurate, it becomes commensurate in the case of $U \geq 8$ at $T = 0.02$, which is consistent with experiments. This change of the shape of $\chi_{\mathbf{q}}^s(0)$ is brought by the deformation of the interacting Fermi surface as shown in Fig. 1, which can not be reproduced by the simple renormalization of t'/t^3 . We also note that the obtained $\chi_{\mathbf{q}}^s(0)$ will be slightly overestimated at low temperatures because its VC's are neglected here.

Next, Fig. 3 (a) shows the imaginary part of the self-energy, $\gamma_{\mathbf{k}} = \text{Im}\Sigma_{\mathbf{k}}(-i0) > 0$, along the Fermi surface for the region $\pi/4 \leq \theta \leq 3\pi/4$ for $T = 0.02, 0.04, \dots, 0.1$.

The definition of the hot spots and the cold spots are given in Fig. 1. In this temperature region, $\gamma_{\mathbf{k}}$ takes the minimum (maximum) value at the the cold spot (hot spot). A hot spot is separated from its counterpart by $\mathbf{Q} = (\pi, \pi)$ in the reciprocal space, and a cold spot is the most distant point from the AF-zone boundary. In the present study, the relations $\gamma_{\text{cold}} \propto T$ and $\gamma_{\text{hot}} \propto \sqrt{T}$ are satisfied because $\xi_{\text{AF}} \lesssim \Delta k^{-1}$ in the FLEX approximation, where Δk is explained in Fig. 1⁹. Note that the damping rate of the quasiparticle is given by $\gamma_{\mathbf{k}}^* = z_{\mathbf{k}} \gamma_{\mathbf{k}}$, where $z_{\mathbf{k}} \equiv (1 - \frac{\partial}{\partial \omega} \text{Re} \Sigma_{\mathbf{k}}(\omega))_{\omega=0}^{-1}$ is the renormalization factor. In the numerical calculation for $U = 9$, $\gamma_{\mathbf{k}}^* \lesssim T$ around the cold spots at lower temperatures because $z_{\mathbf{k}}^{-1} \lesssim 10$ there. Thus, quasiparticle can still be defined.

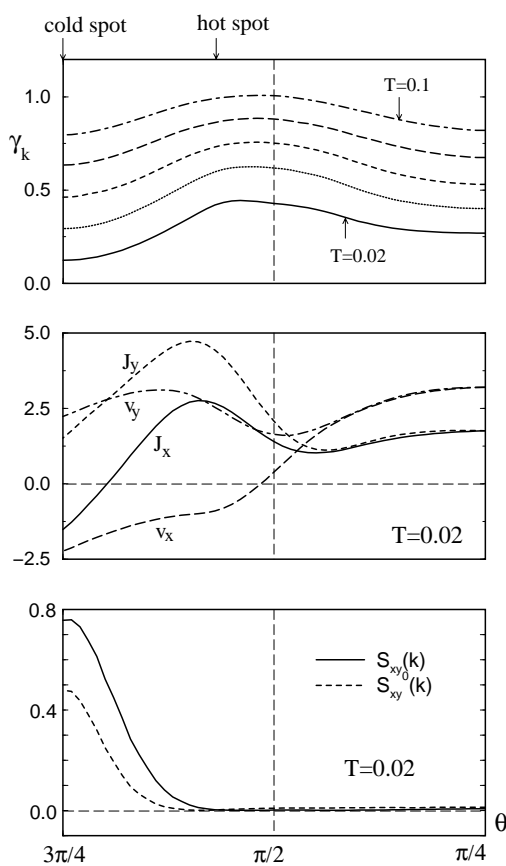


FIG. 3. (a) $\gamma_{\mathbf{k}} = \text{Im} \Sigma_{\mathbf{k}}(-i0)$, (b) $\vec{J}(\mathbf{k}, 0)$ and $\vec{v}(\mathbf{k}, 0)$, (c) $S_{xy}(\mathbf{k})$ and $S_{xy}^0(\mathbf{k})$, along the Fermi surface for the region $\pi/4 \leq \theta \leq 3\pi/4$, for $U = 9$. The locations of the 'hot spot' and the 'cold spot' are introduced in Fig. 1.

III. HALL CONDUCTIVITY BASED ON THE CONSERVATION APPROXIMATION

A. Derivation of the Total Current $\vec{J}_{\mathbf{k}}(\omega)$ Based on the Conservation Approximation

In this section, we calculate both σ_{xx} and $\Delta\sigma_{xy}$ based on the conserving approximation. By using the Kubo formula, they are derived as^{16–18}

$$\sigma_{xx} = e^2 \sum_{\mathbf{k}} \int_{-\infty}^{\infty} \frac{d\epsilon}{\pi} \left(-\frac{\partial f}{\partial \epsilon} \right) (|G_{\mathbf{k}}(\epsilon)|^2 \cdot v_{\mathbf{k}x}(\epsilon) J_{\mathbf{k}x}(\epsilon) - \text{Re}\{G_{\mathbf{k}}^2(\epsilon) \cdot v_{\mathbf{k}x}^2(\epsilon)\}), \quad (6)$$

$$\Delta\sigma_{xy} = -B \cdot e^3 \sum_{\mathbf{k}} \int_{-\infty}^{\infty} \frac{d\epsilon}{2\pi} \left(-\frac{\partial f}{\partial \epsilon} \right) S_{xy}(\mathbf{k}, \epsilon), \quad (7)$$

$$\begin{aligned} S_{xy}(\mathbf{k}, \epsilon) = & |G_{\mathbf{k}}(\epsilon)|^2 \cdot |\text{Im} G_{\mathbf{k}}(\epsilon)| \\ & \times v_{\mathbf{k}x}(\epsilon) \left[J_{\mathbf{k}x}(\epsilon) \frac{\partial J_{\mathbf{k}y}(\epsilon)}{\partial k_y} - J_{\mathbf{k}y}(\epsilon) \frac{\partial J_{\mathbf{k}x}(\epsilon)}{\partial k_y} \right] \\ & + \langle x \leftrightarrow y \rangle, \end{aligned} \quad (8)$$

where $f(\epsilon) = (\exp((\epsilon - \mu)/T) + 1)^{-1}$, and $G_{\mathbf{k}}(\omega + i\delta)$ and $\Sigma_{\mathbf{k}}(\omega + i\delta)$ are derived from $G_{\mathbf{k}}(\omega_n)$ and $\Sigma_{\mathbf{k}}(\omega_n)$ through the numerical analytic continuation. B is the magnetic field parallel to the z -axis. $v_{\mathbf{k}\mu}(\omega) = \frac{\partial}{\partial k_{\mu}} (\epsilon_{\mathbf{k}}^0 + \text{Re} \Sigma_{\mathbf{k}}(\omega))$ is the quasiparticle velocity, and $J_{\mathbf{k}\mu}(\omega)$ is the total current which contains the vertex correction from \mathcal{T}_{22} in the notation of Ref.¹⁶. Later, we examine its importance in detail.

As for the resistivity, the second term of eq. (6) is neglected in the Eliashberg's transport theory, whose derivation is given in §III C. We call it the incoherent part of the conductivity, σ_{inc} , because it is negligible in the case of $\gamma_{\mathbf{k}}^* \ll T$. As a result, these formulae (6)–(9) are valid even for $\gamma_{\mathbf{k}}^* \sim T$.

In the present study, we solve the following Bethe-Salpeter equations for $J_{\mathbf{k}\mu}(\epsilon)$ after the manner of the conserving approximation:

$$\begin{aligned} J_{\mathbf{k}\mu}(\omega) = & v_{\mathbf{k}\mu}(\omega) + \sum_{\mathbf{q}} \int_{-\infty}^{\infty} \frac{d\epsilon}{2\pi} \left[\text{cth} \frac{\epsilon - \omega}{2T} - \text{th} \frac{\epsilon}{2T} \right] \\ & \times \text{Im} V_{\mathbf{k}-\mathbf{q}}(\epsilon - \omega + i\delta) \cdot |G_{\mathbf{k}}(\epsilon)|^2 \cdot J_{\mathbf{q}\mu}(\epsilon), \end{aligned} \quad (9)$$

where we take only the Maki-Thompson (MT) type VC's into account, and neglect the Aslamazov-Larkin (AL) terms because it has little contributions if $\chi_{\mathbf{q}}(0)$ has a sharp peak around $\mathbf{q} = (\pi, \pi)$ ⁹; see Fig. 4. Figure 3 (b) shows the numerical solution of eq. (9). We see that $\vec{J}_{\mathbf{k}}$ is not parallel to $\vec{v}_{\mathbf{k}}$.

On the other hand, in the Boltzmann theory within the relaxation time approximation (RTA), $J_{\mathbf{k}\mu}(\epsilon)$ is simply replaced by $v_{\mathbf{k}\mu}(\epsilon)$ in eqs. (6)–(8). It is an insufficient approximation for the Hall coefficient in nearly AF state as shown in Refs.^{9,10}.

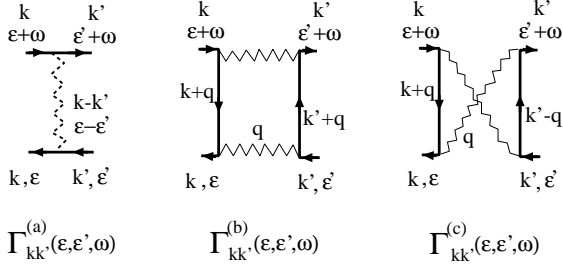


FIG. 4. All the irreducible VC's in the framework of the FLEX approximation: (a) MT-term, and (b,c) AL-terms, respectively.

Now we discuss why \vec{J}_k shows such an anomalous behavior. Here, we choose an arbitrary point on the Fermi surface, \mathbf{k} , which locates between two hot spots in the region $\pi/2 < \theta < \pi$, and also define that $\mathbf{k}' \equiv (k_y, k_x)$. (see Fig. 1.) Then, $\mathbf{k} - \mathbf{k}' \approx (-\pi, \pi)$ is satisfied in the present system, as shown in Fig. 1. In the Bethe-Salpeter eq. (9), \vec{J}_k are strongly connected with $\vec{J}_{k'}$ through $V_{\mathbf{k}-\mathbf{k}'}(\omega)$ in the presence of strong AF fluctuations. Taking this fact into account, the approximate solution of eq. (9) is given by⁹

$$\vec{J}_k = (\vec{v}_k + \alpha_{\mathbf{k}} \vec{v}_{k'}) \cdot (1 - \alpha_{\mathbf{k}}^2)^{-1}, \quad (10)$$

where $\alpha_{\mathbf{k}} = \langle \cos(\theta_J(\mathbf{k}) - \theta_J(\mathbf{q})) \rangle_{|\mathbf{q}-\mathbf{k}| < \xi_{\text{AF}}^{-1}}$, and $\theta_J(\mathbf{q})$ is the angle of $\vec{J}_{\mathbf{q}}$. According to the definition, $\alpha_{\mathbf{k}} < 1$ and $(1 - \alpha_{\mathbf{k}})^{-1} \propto \xi_{\text{AF}}^2$ ⁹. Equation (10) means that J_k at the hot spots will become parallel to the AF zone boundary when ξ_{AF} approaches to infinity. In fact, such a tendency is recognized in Fig. 3 (b). Thus, the anomalous behavior of \vec{J}_k , which is the result of the multiple scattering between \vec{v}_k and $\vec{v}_{k'}$, becomes quite singular when the AF fluctuations are dominant. As a result, the RTA is strongly violated when $\xi_{\text{AF}} \gg 1$ ¹⁹.

Equation (7) is rewritten at low temperatures as

$$\begin{aligned} \Delta\sigma_{xy} &= B \cdot \frac{e^3}{4} \int_{\text{FS}} dk_{\parallel} S_{xy}(k_{\parallel}) \\ S_{xy}(k_{\parallel}) &= (\vec{J}_k \times d\vec{J}_k/dk_{\parallel})_z / \gamma_{\mathbf{k}}^2 \\ &= |\vec{J}_k|^2 (d\theta_J(\mathbf{k})/dk_{\parallel}) / \gamma_{\mathbf{k}}^2, \end{aligned} \quad (11)$$

where $\int_{\text{FS}} dk_{\parallel}$ represents the momentum integration along the Fermi surface, and dk_{\parallel} is parallel to the Fermi surface^{9,10}.

Because $d\alpha_{\mathbf{k}}/dk_{\parallel} = 0$ at the cold spot due to the symmetry of this model, $(\vec{J}_k \times d\vec{J}_k/dk_{\parallel})_z = (1 - \alpha_{\mathbf{k}}^2)^{-1} \cdot (\vec{v}_k \times d\vec{v}_k/dk_{\parallel})_z$ at the cold spot by using eq. (10). Because $\Delta\sigma_{xy}$ is given mainly around the cold spots in the k_{\parallel} -integration of eq. (11), we conclude the relation

$$\Delta\sigma_{xy}/\Delta\sigma_{xy}^0 \propto \xi_{\text{AF}}^2 \propto T^{-1} \quad (12)$$

in the presence of the strong AF fluctuations. Here $\Delta\sigma_{xy}^0$ is given by replacing $\vec{J}_k(\omega)$ with $\vec{v}_k(\omega)$ in eq.(7), which is

equal to the result of the RTA. As for $\Delta\sigma_{xy}^0$, the conventional Kohler's rule $\Delta\sigma_{xy}^0 \propto (\sigma_{xx})^2$ is well satisfied in the present calculation because the anisotropy of $\gamma_{\mathbf{k}}$ is not so extreme. ($\gamma_{\text{hot}}/\gamma_{\text{cold}}$ is at most 3.) As a result, eq. (12) leads the relation $R_H \equiv (\Delta\sigma_{xy}/B) \cdot \rho^2 \propto \xi_{\text{AF}}^2 \propto T^{-1}$, which is recognized in the present numerical calculations as shown below.

The above analysis is confirmed by the numerical results of $S_{xy}(k_{\parallel})$ in Fig. 3 (c). $S_{xy}^0(k_{\parallel})$ is given by the RTA. The dominant contributions to $\Delta\sigma_{xy}$ come from the region around the cold spot, $S_{xy}(k_{\parallel})$ for region $\pi/4 < \theta < \pi/2$ is considerably small because the curvature of the Fermi surface is very small there. In the present case, both $S_{xy}^0(k_{\parallel})$ and $S_{xy}(k_{\parallel})$ are positive everywhere. It is not the case for high- T_c cuprates; for example, the change of the sign of R_H is realized in Nd-compounds^{9,10}.

B. Numerical Results for Transport Phenomena

Now, we study both ρ and R_H for various values of U , because the main effect of the applied pressure is expected to increase the bandwidth W_b , in other words, to reduce the value of U/W_b ¹¹. At the same time, the value of t'/t may be also modified by pressure. This effect is not discussed here although the electronic states are sensitive to t'/t according to the FLEX approximation³.

Figure 5 (a) shows the temperature dependences of the resistivity $\rho = 1/\sigma_{xx}$. All the ρ 's show the approximate T -linear resistivity, reflecting the T -linear behavior of γ_{cold} . At the same temperature, ρ increases monotonously as U increases. Here, $\rho_0 = 1/\sigma_{xx}^0$ is the resistivity without the VC's, which is given by replacing $\vec{J}_k(\omega)$ with $\vec{v}_k(\omega)$ in eq. (6). We see that $\rho > \rho_0$ due to the VC's for the current.

Here, we comment on the anisotropy of ρ . In the present model, $\sigma_{\mu\mu}$ depends on the angle of the μ -axis because there is no four-fold rotational symmetry in this system. We find that ρ takes its maximum (minimum) value along the $(\theta = \pi/4)$ -axis ($(\theta = 3\pi/4)$ -axis), and $\rho_{\text{max}}/\rho_{\text{min}} \approx 1.6$ with weak temperature dependence.

Next, we discuss on the Hall coefficient R_H . As shown in Fig. 5 (b), R_H follows the Curie-Weiss like temperature dependence, which is consistent with the relation (12). Actually, both $\xi_{\text{AF}}^2 \propto \chi_Q(0)$ and R_H increase monotonously as U increases at the same temperatures. (see Fig. 2.) As a result, the large temperature dependence of R_H in κ -(BEDT-TTF)₂X salts is reproduced well by taking account of the VC's for the current.

To see the importance of the VC's, we also show $R_H^0 = (\Delta\sigma_{xy}^0/B) \cdot \rho_0^2$, which is the result of the RTA: We see that R_H^0 is nearly constant, and $R_H \approx R_H^0$ at higher temperatures ($T \gtrsim 0.1$) because of $\vec{J}_k \approx \vec{v}_k$ in this case. We note that dR_H^0/dT is slightly positive for $T > 0.05$, because the curvature of the Fermi surface around the cold spot decreases as T decreases due to the

growth of the AF fluctuations. (see Fig. 1.) Whereas $dR_H^0/dT < 0$ for $T < 0.05$ because of the rapid increase of the anisotropy of $\gamma_{\mathbf{k}}$ at lower temperatures. However, this increase of R_H^0 is too small to explain experimental results.

Finally, we show $\cot\theta_H = \sigma_{xx}/\Delta\sigma_{xy}$ in Fig. 5 (c). All the $\cot\theta_H$'s are approximately proportional to T^2 below $T \lesssim 0.05$, where both $R_H \propto T^{-1}$ and $\rho \propto T$ are satisfied approximately. This result is highly consistent with experiments reported in Ref.⁷. Similar behavior of $\cot\theta_H$ is also observed in high- T_c cuprates. For high- T_c cuprates, Anderson claimed that it suggests the non-Fermi liquid ground state which possesses two kinds of relaxation rates²⁰. However, we stress that the relation $\cot\theta_H \propto T^2$ is naturally understood both for κ -(BEDT-TTF)₂X salts and for high- T_c cuprates within the framework of the nearly AF Fermi liquid.

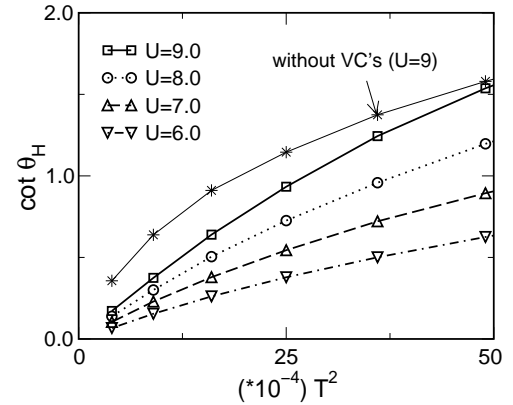
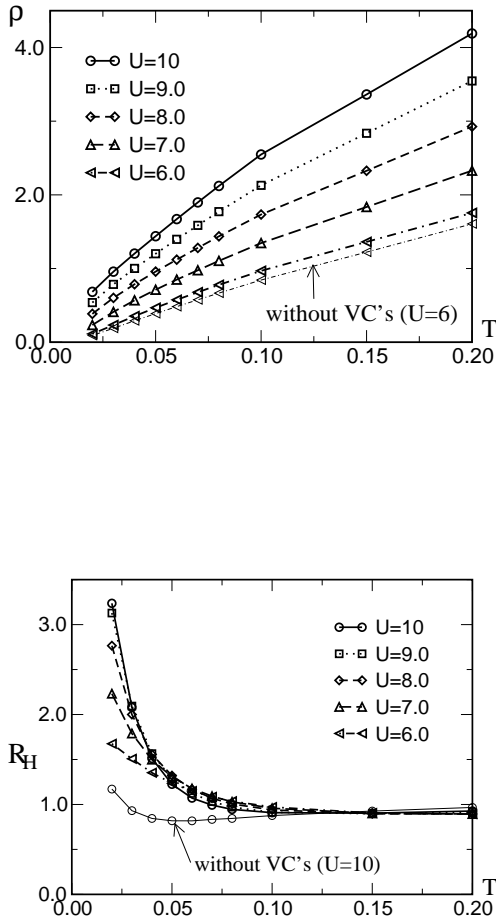


FIG. 5. The temperature dependence of (a) ρ , (b) R_H , and (c) the $\cot\theta_H$ for $U = 6 \sim 10$. We put $e = 1$ and $\hbar = 1$. $T = 0.1$ corresponds to 100K approximately.

Finally, we discuss the U -dependence of ρ and R_H in the present calculations, and compare them with the experimental pressure dependences. According to the experiments on $X = \text{Cu}[\text{N}(\text{CN})_2]\text{Cl}$ ⁷, as the applied pressure increases, (i) ρ decreases monotonously, (ii) R_H is almost unchanged, and (iii) $\cot\theta_H$ decreases monotonously. The effect of the applied pressure is to increase W_b while U is unchanged, i.e., to decrease U/W_b . Moreover, on condition that U/W_b is constant, it is easy to see that $\rho \propto W_b^{-1}$, $R_H \propto W_b^0$, and $\cot(\theta_H) \propto W_b^{-1}$. As a result, the obtained U -dependence of ρ and $\cot\theta_H$, which are shown in Fig. 5 (a) and (c), are consistent with experiments. On the other hand, the observed weak pressure dependence of R_H will correspond to the behavior for $U \geq 8$ in Fig. 5 (b). In conclusion, experimentally observed pressure effects (i)-(iii) are reproduced in our study.

At last, we comment on the superconductivity: We find $T_c = 0.024$ for $U = 9$ and $T_c = 0.004$ for $U = 5$ by solving the Eliashberg equations. This is consistent with the decrease of T_c under pressure observed experimentally. Roughly speaking, $T = 0.01$ corresponds to 10K because the band-width $W_{\text{band}} \sim 0.5\text{eV}$ at ambient pressure. Although the obtained T_c 's is rather higher than experimental one's, it decreases if we put t'/t larger than 0.7³.

C. Derivation of σ_{inc}

In this subsection, we give the derivation of the second term of eq. (6) based on the Fermi liquid theory. We call it the incoherent part of the conductivity σ_{inc} because it gives negligible contribution when the quasiparticles are well-defined. We call the first term of eq. (6) the coherent part of the conductivity σ_{coh} , which was derived by Eliashberg under the assumption $\gamma_{\mathbf{k}}^* \ll T^{16}$.

According to the Kubo formula, the conductivity is expressed by the retarded two-particle Green function $K^R(\omega)$, whose explicit form within the Fermi liquid theory is given by eq.(9) of Ref.¹⁶. The first term of eq. (6), which was derived by Eliashberg, comes from the coherent terms of $K^R(\omega)$ which include at least one $g_2 = G^R G^A$. Here, we study the contribution from the incoherent part without g_2 , $K_{\text{inc}}^R(\omega)$, which has not been analyzed previously. Hereafter, we omit the momentum variables for simplicity. $K_{\text{inc}}^R(\omega)$ is given as follows:

$$K_{\text{inc}}^R(\omega) = - \sum_{i=1,3} \int \frac{d\epsilon}{4\pi i} v_{\mathbf{k}x}^0 \lambda_i(\epsilon; \omega) g_i(\epsilon; \omega) \Lambda_x^i(\epsilon; \omega), \quad (13)$$

$$\begin{aligned} \Lambda_x^i(\epsilon; \omega) &= v_{\mathbf{k}x}^0 + \sum_{j=1,3} \int \frac{d\epsilon'}{4\pi i} \mathcal{T}_{i,j}(\epsilon, \epsilon'; \omega) \\ &\quad \times g_j(\epsilon'; \omega) \Lambda_x^j(\epsilon'; \omega), \end{aligned} \quad (14)$$

which is shown in Fig. 6(a). Here, $g_1(\epsilon; \omega) = G_{\mathbf{k}}(\epsilon + \omega + i\delta) G_{\mathbf{k}}(\epsilon + i\delta)$, $g_3(\epsilon; \omega) = \{g_1(\epsilon; \omega)\}^*$, $\lambda_1(\epsilon; \omega) = \text{th}(\epsilon/2T)$, $\lambda_3(\epsilon; \omega) = -\text{th}((\epsilon + \omega)/2T)$, and $v_{\mathbf{k}x}^0 = d\epsilon^0/dk_x$, respectively. The quantities $\mathcal{T}_{i,j}(\epsilon, \epsilon'; \omega)$ are given by the product of irreducible four-point vertices $\Gamma_{i,j}^{\text{I}(\text{II})}(\epsilon, \epsilon'; \omega)$ and thermal factors brought by the analytic continuation, whose definition is given by eq. (12) of Ref.¹⁶. (Hereafter, all the four-point vertices are 'irreducible' with respect to g_i .) We study the conductivity from the incoherent terms, given by $\sigma_{\text{inc}} = e^2 \lim_{\omega \rightarrow 0} \text{Im}K_{\text{inc}}^R(\omega)/\omega$, and find that it gives a finite contribution when the life-time of the quasiparticles becomes shorter.

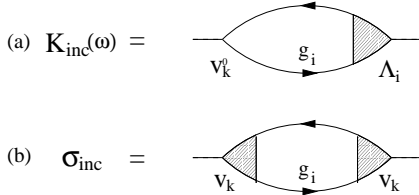


FIG. 6. The diagrams for (a) $K_{\text{inc}}(\omega)$, and for (b) σ_{inc} , respectively.

Now, we derive the ω -linear term of $\text{Im}K_{\text{inc}}^R(\omega)$. $\mathcal{T}_{i,3}(\epsilon, \epsilon'; \omega)$ ($i = 1, 3$) contains the thermal factors $\text{th}((\epsilon + \omega)/2T)$ as shown in eq. (12) of Ref.¹⁶. We can check that $K_{\text{inc}}^R(\omega)$ given by eqs. (13) and (14) becomes real quantity when we put $\omega = 0$ (i) in all the factors $\text{th}((\epsilon + \omega)/2T)$ and (ii) in all the irreducible vertices $\Gamma_{i,j}(\epsilon, \epsilon'; \omega)$, by taking account of the relation $\Gamma_{i,j}^{\text{I}(\text{II})}(\epsilon, \epsilon'; 0) = \{\Gamma_{4-i,4-j}^{\text{I}(\text{II})}(\epsilon, \epsilon'; 0)\}^*$ for $i, j = 1, 3$. This means that the ω -linear term of $\text{Im}K_{\text{inc}}^R(\omega)$ comes only from one of (i) or (ii). Because $\Lambda_x^i(\epsilon; \omega)$ contains infinite number of $\mathcal{T}_{i,j}$ ($i, j = 1, 3$), we find that

$$\sigma_{\text{inc}} = -e^2 \int_{-\infty}^{\infty} \frac{d\epsilon}{\pi} \left(-\frac{\partial f}{\partial \epsilon} \right) \text{Re} \left\{ \tilde{\Lambda}_x^1(\epsilon; 0) g_1(\epsilon; 0) \Lambda_x^1(\epsilon; 0) \right\}$$

$$\begin{aligned} &- e^2 \iint_{-\infty}^{\infty} \frac{d\epsilon d\epsilon'}{4\pi^2} \sum_{i,j=1,3} \lambda_i(\epsilon; 0) \tilde{\Lambda}_x^i(\epsilon; 0) g_i(\epsilon; 0) \\ &\quad \times \tilde{\mathcal{T}}_{i,j}(\epsilon, \epsilon') g_j(\epsilon'; 0) \Lambda_x^j(\epsilon'; 0) \end{aligned} \quad (15)$$

where $\tilde{\mathcal{T}}_{i,j}(\epsilon, \epsilon')$ is defined as the $i\omega$ -derivation of the vertex part ($\Gamma_{i,j}$) of $\mathcal{T}_{i,j}(\epsilon, \epsilon'; \omega)$, and put $\omega = 0$.

As for the second term of (15), $\tilde{\mathcal{T}}_{i,j}(\epsilon, \epsilon')$ given by the MT-term vanishes identically. On the other hand, the two AL-terms causes the finite contribution for $\text{Im}K_{\text{inc}}^R(\omega)$. After the long calculation, $\tilde{\mathcal{T}}_{1,1}(\epsilon, \epsilon')$ in the FLEX approximation is given by

$$\tilde{\mathcal{T}}_{1,1}(\mathbf{k}\epsilon, \mathbf{k}'\epsilon') = \bar{\Gamma}_{1,1}^{\text{I}}(\mathbf{k}\epsilon, \mathbf{k}'\epsilon') \cdot \text{th}(\epsilon'/2T), \quad (16)$$

$$\begin{aligned} \bar{\Gamma}_{1,1}^{\text{I}}(\mathbf{k}\epsilon, \mathbf{k}'\epsilon') &= - \sum_{\mathbf{q}} \mathcal{P} \int_{-\infty}^{\infty} \frac{dz}{2\pi} \frac{\partial \text{cth}(z/2T)}{\partial z} \pi^2 \\ &\quad \times \rho_{\mathbf{q}}(\epsilon' + z) (\rho_{\mathbf{k}-\mathbf{k}'+\mathbf{q}}(\epsilon + z) - \rho_{\mathbf{k}-\mathbf{k}'+\mathbf{q}}(\epsilon - z)) \\ &\quad \times (3U^4/2) \cdot [\text{Im}\chi_{\mathbf{k}-\mathbf{k}'}^s(-z + i\delta)]^2, \end{aligned} \quad (17)$$

where we have used the relation $v_{\mathbf{k}} = -v_{-\mathbf{k}}$ in derivation, and $\rho_{\mathbf{k}}(\omega) = -\text{Im}G_{\mathbf{k}}(\omega + i\delta)/\pi$. Other terms which do not contribute to σ_{inc} are dropped in eq. (17). In the same way of deriving eq. (17), we can show that $\tilde{\mathcal{T}}_{i,j}(\mathbf{k}\epsilon, \mathbf{k}'\epsilon') = (-1)^{(j-1)/2} \cdot \tilde{\mathcal{T}}_{1,1}(\mathbf{k}\epsilon, \mathbf{k}'\epsilon')$ for $i, j = 1, 3$.

Now, we show that the second term of eq. (15) is negligible: It vanishes at $T = 0$ because Equation (17) vanishes in this case. (Note that $\text{Im}\chi_{\mathbf{k}}^s(0) = 0$.) It should be much small even at finite temperatures because of the cancellation caused by the factor $(\rho(\epsilon + z) - \rho(\epsilon - z))$ in eq. (17). By this reason, we consider only the first term of eq. (15) hereafter.

As for Λ_x in eq. (15), we can show that

$$\begin{aligned} \text{Re}\{\tilde{\Lambda}_x^1(0; 0) - \Lambda_x^1(0; 0)\} &= \\ \frac{1}{2} \sum_{i,j=1,3} \int \frac{d\epsilon}{4\pi i} \left[\text{cth} \frac{\epsilon}{2T} - \text{th} \frac{\epsilon}{2T} \right] (-1)^{(j-1)/2} \\ &\quad \times (\Gamma_{i,j}^{\text{II}}(0, \epsilon; 0) - \Gamma_{i,j}^{\text{I}}(0, \epsilon; 0)) g_j(\epsilon) v_{\mathbf{k}x}^0, \end{aligned} \quad (18)$$

which is proportional to T^2 at low temperatures. (Here, $\Gamma_{i,j}^{\text{I},\text{II}}$ is reducible with respect to g_i .) Thus, $\tilde{\Lambda}_x^1(0; 0)$ approximately identical to $\Lambda_x^1(0; 0)$. We have also estimated eq. (18) numerically by taking only the MT terms into account, and find that the difference between them is at most a few percent.

In conclusion, we get the following expression for σ_{inc} :

$$\begin{aligned} \sigma_{\text{inc}} &= -e^2 \sum_{\mathbf{k}} \int_{-\infty}^{\infty} \frac{d\epsilon}{\pi} \left(-\frac{\partial f}{\partial \epsilon} \right) \\ &\quad \times \text{Re}\{ G_{\mathbf{k}}^2(\epsilon + i\delta) \cdot v_{\mathbf{k}x}^2(\epsilon + i\delta) \}, \end{aligned} \quad (19)$$

which is shown in Fig. 6(b). Here we have used the Ward identity $\Lambda_x^1(\epsilon; 0) = v_{\mathbf{k}x}^0 + \frac{\partial}{\partial k_x} \Sigma_{\mathbf{k}}(\epsilon + i\delta) \equiv v_{\mathbf{k}x}(\epsilon + i\delta)$. Note that the vertex correction, given by the momentum derivative of $\Sigma_{\mathbf{k}}(\omega)$ appears twice in eq. (19). Thus the obtained σ_{inc} gives the second term of eq. (6).

If we can put $G_{\mathbf{k}}(\epsilon) = z_{\mathbf{k}}/(\epsilon + \mu - \epsilon_{\mathbf{k}}^* + i\gamma_{\mathbf{k}}^*)$, eq. (19) becomes

$$\sigma_{\text{inc}} = e^2 \sum_{\mathbf{k}} \int \frac{d\epsilon}{\pi} \left(-\frac{\partial f}{\partial \epsilon} \right) z_{\mathbf{k}}^2 \frac{-(\epsilon - \epsilon_{\mathbf{k}}^*)^2 + \gamma_{\mathbf{k}}^{*2}}{((\epsilon - \epsilon_{\mathbf{k}}^*)^2 + \gamma_{\mathbf{k}}^{*2})^2} v_{\mathbf{k}x}^2, \quad (20)$$

where $\gamma_{\mathbf{k}}^* = z_{\mathbf{k}}\gamma_{\mathbf{k}}$ and $\epsilon_{\mathbf{k}}^* = z_{\mathbf{k}}\epsilon_{\mathbf{k}}$, respectively. In the case of $\gamma_{\mathbf{k}}^* \ll T \ll W_b$, $\sigma_{\text{inc}} \approx 0$ is realized according to eq.(20), while $\sigma_{\text{coh}} \propto \gamma_{\text{cold}}^{-1}$. However, such a condition is not satisfied in the present calculation as shown in Fig. 3(a). At lower temperatures, $\gamma_{\mathbf{k}}^* \lesssim T$ is satisfied because $z_{\mathbf{k}}^{-1} \lesssim 10$ then, whereas $\gamma_{\mathbf{k}}^* \gtrsim T$ at higher temperatures because $z_{\mathbf{k}}^{-1}$ decreases as T increases. Thus, σ_{inc} is expected to be important at higher temperatures. In Appendix A, we show its importance numerically.

IV. COMPARISON WITH EXPERIMENTS

A. Effect of Band-Splitting around the Hot-Spots

In this section, we compare our theoretical results with experiments in more detail. Here, we discuss the validity of the present results based on the effective model shown in Fig. 1. Precisely speaking, in many (not all) real κ -(BEDT-TTF)₂X compounds, the Fermi surface splits slightly around the hot spots in Fig. 1 because a unit cell contains two dimers of the BEDT-TTF molecules (see Appendix B). In this sense, the present model may be too simplified for the quantitative studies.

However, the mechanism of the enhancement of R_H due to the AF fluctuations proposed in this paper is surely valid because only the quasiparticles around the cold spots plays an important role for transport phenomena as shown in Fig. 3. On the other hand, R_H at higher temperatures may be affected by the splitting of the Fermi surface at the hot spots. Thus, our calculation based on the dispersion, eq. (1), is comparable with experiments at least in the lower temperature region.

B. Effect of Temperature Dependence of the Volume

Next, we discuss the effect of the thermal contraction of the volume, which is known to be quite large in various organic metals.^{21,22} For example, (TMTSF)₂PF₆ at ambient pressure shows $\rho \propto T^n$ and $n \approx 2$, whereas $n \approx 1$ is concluded after the effect of the thermal contraction is compensated²².

As for X=Cu[N(CN)₂]Cl, $\rho \propto T^n$ and $n \approx 2$ is observed below 100K at nearly ambient pressures^{1,23}. However, $n \approx 1$ is realized qualitatively under the constant-volume condition according to Ref.⁷: In the article, the authors used the piston-cylinder clamped cell to make pressure, and the oil inside of the cell freezes at ~ 200 K, which make the volume of the sample constant²⁴. This

experimental fact means that $n \approx 2$ at ambient pressure should not be interpreted as the conventional Fermi liquid behavior. Note that the non-Fermi liquid behavior $n \approx 1$ is observed under pressure, nonetheless U/W_b decreases by pressure²⁵.

Thus, the results obtained in our study, $\rho \propto T$ and $R_H \propto T^{-1}$, are qualitatively consistent with Ref.⁷, which are expected to be the intrinsic behaviors in κ -BEDT-TTF compounds without the volume contraction. We stress that, as for organic compounds, the measurements under constant volume condition are highly demanded for the comparison with theories.

C. The Saturation of R_H at Lower Temperatures

Here, we comment on the saturation of R_H below a characteristic temperature T^* observed experimentally. Around $T \approx T^*$, the $1/T_1T$ also saturates and begins to decrease below T^* , which is called the pseudo spin-gap behavior. This results suggests that ξ_{AF}^2 , or $\chi_Q^s(0)$, will saturates below T^* . (We note that many experiments for $1/T_1T$ are done at ambient pressure, so the volume contraction effect may play some quantitative effect on $1/T_1T$ at low temperatures.) Thus, the analytical relation in our work, $R_H \propto \xi_{\text{AF}}^2$, is consistent with these experiments.

However, R_H of our numerical calculation in Figs. 5 does not saturate: This is because the FLEX approximation does not reproduce the saturation of ξ_{AF}^2 below T^* , which is a significant future problem. One of the possible mechanism for it will be the precursor effect of superconductivity below T^* ²⁶. Finally, we point out that R_H begins to decrease on cooling below T^* in under-doped high- T_c cuprates, whereas it takes a saturate value at lower temperatures in X=Cu[N(CN)₂]Cl⁷.

V. CONCLUSIONS

In this paper, we have presented the theoretical study for the resistivity and the Hall coefficient of the κ -(BEDT-TTF)₂X salts. Reference⁷ point out some experimental evidences that there anomalous behaviors have close connection with the grows of the AF fluctuations²⁷. According to our theory, the Hall coefficient follows the relation $R_H \propto \xi_{\text{AF}}^2 \propto T^{-1}$ in nearly AF Fermi liquid state, which is consistent with the experiment under the constant volume condition⁷. This anomaly of R_H , which can not be reproduced by the RTA, is found to come from the VC's for the current which is indispensable to satisfy the conserving laws.

Moreover, based on the Kubo formula, we have derived the expression of the incoherent conductivity σ_{inc} beyond the Eliashberg's transport theory, and found that it give a qualitatively important contribution in κ -(BEDT-TTF)₂X and in high- T_c cuprates at higher temperatures,

where $\gamma_{\mathbf{k}}^* \sim T$ is realized. It also give the appropriate temperature dependence of R_H .

We have calculated both ρ and R_H based on the FLEX approximation for $U = 6 \sim 10$, without assuming any fitting parameters. The obtained U -dependences for ρ , R_H and $\cot\theta_H$ explain well the experimentally observed pressure dependences. In conclusion, many essential electronic properties of κ -(BEDT-TTF)₂X, especially both the anomalies of transport phenomena and the phase diagram, are explained well from the standpoint of the nearly AF Fermi liquid state. We stress that further observations under the constant volume condition are highly demanded for organic metals to make a meaningful comparison between theory.

ACKNOWLEDGMENTS

We are grateful to T. Moriya, K. Yamada, K. Ueda, and K. Kanki for valuable comments and discussions. We also thank Murata and Y. Nogami for the important information on experiments.

APPENDIX A: IMPORTANCE OF THE INCOHERENT CONDUCTIVITY

In this appendix, we numerically show the important role of σ_{inc} to get the reasonable behaviors of ρ and R_H . Figure 7 shows the temperature dependence of the Hall coefficient and the resistivity. $\rho = 1/(\sigma_{\text{coh}} + \sigma_{\text{inc}})$, $\rho' = 1/\sigma_{\text{coh}}$ and $\rho_{\text{RTA}} = 1/\sigma_{\text{RTA}}$, respectively. Here, σ_{RTA} is given by replacing $J_{\mathbf{k}}$ with $v_{\mathbf{k}}$ in σ_{coh} , which is equal to the result from the relaxation time approximation. We find that (i) $\rho' > \rho_{\text{RTA}}$ because of the VC's for the current, and (ii) $\rho < \rho'$ because of σ_{inc} , which becomes dominant especially at higher temperatures. As a result, $\rho < \rho_{\text{RTA}}$ is realized at higher temperatures.

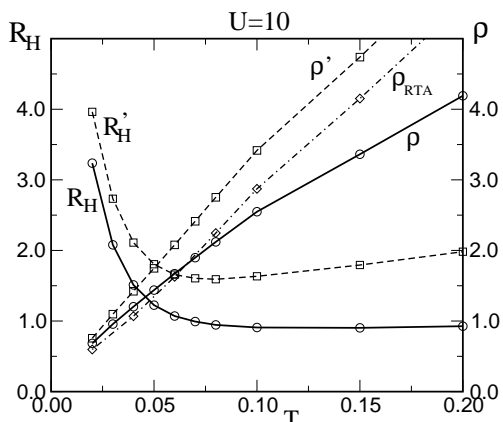


FIG. 7. (i) Comparison between $\rho = 1/(\sigma_{\text{coh}} + \sigma_{\text{inc}})$ and $\rho' = 1/\sigma_{\text{coh}}$ for $U = 10$. ρ becomes smaller than ρ' because of the incoherent part of the resistivity. ρ_{RTA} is given by the RTA. (ii) Comparison between $R_H = (\Delta\sigma_{xy}/B) \cdot \rho^2$ and $R'_H = (\Delta\sigma_{xy}/B) \cdot \rho'^2$ for $U = 10$. We see that dR'_H/dT becomes positive below $T \approx 0.08$, which is inconsistent with experiments.

As for Hall effect, $R_H = (\Delta\sigma_{xy}/B) \cdot \rho^2$ and $R'_H = (\Delta\sigma_{xy}/B) \cdot \rho'^2$, respectively. We see that $R_H < R'_H$ because $\rho < \rho'$. However, $R_H(T = 0.02)/R_H(T = 0.2)$ is larger than that of R'_H , so the incoherent conductivity make the temperature dependence of R_H larger. We stress that dR'_H/dT become positive at higher temperature, which contradicts with experiments⁷. In conclusion, we find that σ_{inc} is necessary to reproduce the reasonable behavior of R_H .

APPENDIX B: THE MORE PRECISE TIGHT-BINDING MODEL FOR κ -(BEDT-TTF)₂X

In real κ -(BEDT-TTF)₂X systems, there are two pairs of closely-packed BEDT-TTF molecules in a unit cell, and only the bonding-orbit of each closely-packed molecules contributes to make the Fermi surface. By taking the results of the band-calculations into account, we get the effective tight-binding model for κ -(BEDT-TTF)₂X as shown in Fig. 8, where there are two sites (a,b) in a unit cell. Each site corresponds to a closely-packed BEDT-TTF molecules. This model becomes equal to the anisotropic triangular lattice model given by Fig. 1 if we put $t_1 = t'_1 = t_2 = t'_2 \equiv t$ and $t_3 \equiv t'$.

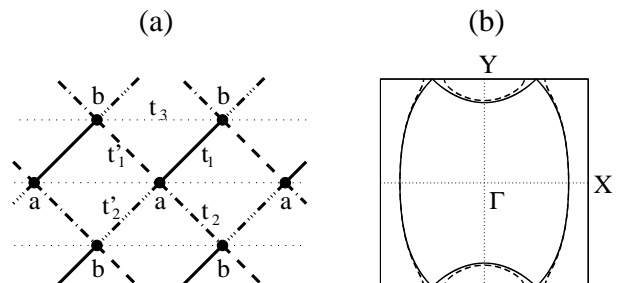


FIG. 8.

(a): The effective model for κ -(BEDT-TTF) salts with two-sites in a unit cell (a, b). The hopping parameters of this model are given by the parameters in Fig.1 of Ref.¹¹ as $t_1 = (p+q')/2$, $t'_1 = (p+q)/2$, $t_2 = (p'+q)/2$, $t'_2 = (p'+q')/2$, and $t_3 = b_2/2$, respectively. (b): The Fermi surface for $t_1 = t'_1 = t_2 = t'_2 = 1$ (full line), and for $t_1 = t'_2 = 1.1$ and $t_2 = t'_1 = 0.9$ (broken line), respectively. In both cases, $t_3 = 0.7$. Note that the former is equivalent to Fig.1 in the extended zone representation.

The dispersion of the tight-binding model given by Fig. 8 for $U = 0$ is derived as $\epsilon_{\mathbf{k}}^{\pm} = 2t_3 \cos k_y \pm [t_1^2 + t_1'^2 + t_2^2 + t_2'^2 + 2(t_1 t_1' + t_2 t_2') \cos k_y + 2(t_1' t_2 + t_1 t_2') \cos k_x + 2t_1 t_2' \cos(k_x + k_y) + 2t_1' t_2 \cos(k_x - k_y)]^{1/2}$. When $|k_y| = \pi$, then $\epsilon_{\mathbf{k}}^+ - \epsilon_{\mathbf{k}}^- = 2[(t_1 - t_1')^2 + (t_2 - t_2')^2]^{1/2}$. This means that the Fermi surface splits around the hot spots when $t_1 \neq t_1'$ or $t_2 \neq t_2'$, which is realized in many systems. (However, both $t_1 = t_1'$ and $t_2 = t_2'$ are satisfied exactly in some compounds exceptionally, e.g.,²⁸.) This splittings of the Fermi surface at the hot spots will not affect the temperature dependence of R_H at low temperatures, as discussed in §III.

¹ K. Kanoda: *Physica C* **282-287** (1997) 299.
² A. Kawano, K. Miyagawa, Y. Nakazawa and K. Kanoda: *Phys. Rev. B* **52** (1995) 15 522.
³ H. Kino, and H. Kontani: *J. Phys. Soc. Jpn.* **67** 3691 (1998).
⁴ H. Kondo and T. Moriya: *J. Phys. Soc. Jpn.* **67** 3695 (1998).
⁵ J. Schmalian: *Phys. Rev. Lett.* **81** (1998) 4232.
⁶ H. Kondo and T. Moriya: *J. Phys. Soc. Jpn.* **68** (1999).
⁷ Yu. V. Sushko, N. Shirakawa, K. Murata, Y. Kubo, N.D. Kushch, E.B. Yagubskii: *Synth. Met.* **85** (1997) 1541.
⁸ K. Murata, M. Ishibashi, Y. Honda, N.A. Fortune, M. Tokumoto, N. Kinoshita and H. Anzai: *Solid State Comm.* **76** (1990) 377.
⁹ H. Kontani, K. Kanki and K. Ueda: *Phys. Rev. B* **59** (1999) 14723.
¹⁰ K. Kanki and H. Kontani: *J. Phys. Soc. Jpn.* **68**, (1999) 1614.
¹¹ H. Kino and H. Fukuyama: *J. Phys. Soc. Jpn.* **65** (1996)

2158, and references therein.
¹² N. E. Bickers et al. : *Phys. Rev. Lett.* **62** (1989) 961.
¹³ P. Monthoux and D. J. Scalapino: *Phys. Rev. Lett.* **72** (1994) 1874.
¹⁴ T. Dahm and L. Tewordt: *Phys. Rev. B* **52** (1995) 1297.
¹⁵ H. Kontani and K. Ueda: *Phys. Rev. Lett.* **80** (1998) 5619.
¹⁶ G. M. Eliashberg : *Sov. Phys. JETP* **14** (1962), 886.
¹⁷ H. Kohno and K. Yamada: *Prog. Theor. Phys.* **80** (1988) 623.
¹⁸ H. Fukuyama, H. Ebisawa and Y. Wada: *Prog. Theor. Phys.* **42** (1969) 494.
¹⁹ According to the analysis, $\vec{J}_{\mathbf{k}}$ becomes parallel to the magnetic Brillouin zone at the hot spot when $\xi_{\text{AF}} \rightarrow \infty$, which may be interpreted as the precursor effect of the AF ordered state.
²⁰ P.W. Anderson: *Phys. Rev. Lett.* **67** (1991) 2092.
²¹ M. Watanabe, Y. Nogami, K. Oshima, H. Ito, T. Ishiguro and G. Saito: accepted in *Synth. Met.*
²² C. Bourbonnais and D. Jérôme: *cond-mat/9903101*, D. Jérôme, P. Auban-Senzier, L. Balicas, K. Bahnia, W. Kang, P. Wzieter, C. Berther, P. Caretta, M. Horvatic, P. Segransan, L. Hubert and C. Bourbonnais: *Synth. Met.* **70** (1995) 719.
²³ M. Dressel eq al.: *Synth. Metals.* **85** (1997) 1503.
²⁴ K. Murata: private communication.
²⁵ When $\rho \propto T^2$ is observed in $\kappa\text{-}(BEDT-TTF)_2X$ compounds, in general, (i) the volume contraction is prominent, and (ii) ρ shows an insulating behavior at higher temperatures.
²⁶ T. Jujo and K. Yamada: *J. Phys. Soc. Jpn.* **68** (1999) 2198.
²⁷ The experimentally observed 'positive magnetoresistance' is also reproduced by the VC's theoretically if the AF fluctuations are dominant [H. Kontani: unpublished].
²⁸ e.g., T. Komatsu, N. Matsukawa, T. Inoue and G. Saito: *J. Phys. Soc. Jpn.* **65** (1996) 1340: The overlap integrals are also listed for a number of $\kappa\text{-}(BEDT-TTF)_2X$ salts and related materials.